

Pose Tracking Without Linear- and Angular-Velocity Feedback Using Dual Quaternions

NUNO FILIPE
 ALFREDO VALVERDE
 PANAGIOTIS TSIOTRAS, Senior Member, IEEE
 Georgia Institute of Technology
 Atlanta, GA, USA

Since vision-based sensors typically cannot directly measure the relative linear and angular velocities between two spacecraft, it is useful to develop attitude- and position-tracking controllers—namely, pose-tracking controllers—that do not require such measurements. Using dual quaternions and based on an existing attitude-only tracking controller, a pose-tracking controller that does not require relative linear- or angular-velocity measurements is developed in this paper. Compared to the existing literature, this velocity-free pose-tracking controller guarantees that the pose of the chaser spacecraft will converge to the desired pose independent of the initial state, even if the reference motion is not sufficiently exciting. In addition, the convergence region does not depend on the gains chosen by the user. The velocity-free controller is verified and compared with a velocity-feedback controller through two simulations. In particular, the proposed velocity-free controller is compared qualitatively and quantitatively with a velocity-feedback controller and an extended Kalman filter using a relatively realistic satellite proximity-operation scenario.

Manuscript received January 22, 2015; revised June 29, 2015; released for publication July 5, 2015.

DOI. No. 10.1109/TAES.2015.150046.

Refereeing of this contribution was handled by J. Li.

This work was supported by an International Fulbright Science and Technology Award sponsored by the Bureau of Educational and Cultural Affairs of the U.S. Department of State, Air Force Research Laboratory (AFRL) research award FA9453-13-C-0201, and National Science Foundation (NSF) award NRI-142645.

Authors' address: Georgia Institute of Technology, Daniel Guggenheim School of Aerospace Engineering, 270 Ferst Drive NW, Atlanta, GA 30332-0150, E-mail: (nunoaero@gmail.com).

0018-9251/16/\$26.00 © 2016 IEEE

NOMENCLATURE

$0_{m \times n}$	$m \times n$ matrix of 0s
$I_{n \times n}$	$n \times n$ identity matrix
1	Quaternion (1, $0_{3 \times 1}$)
0	Quaternion (0, $0_{3 \times 1}$)
$q_{Y/Z}$	Unit quaternion from the Z-frame to the Y-frame
$\bar{\omega}_{Y/Z}^X$	Angular velocity of the Y-frame with respect to the Z-frame expressed in the X-frame
$\bar{v}_{Y/Z}^X$	Linear velocity of the origin of the Y-frame with respect to the Z-frame expressed in the X-frame
$\bar{r}_{Y/Z}^X$	Translation vector from the origin of the Z-frame to the origin of the Y-frame expressed in the X-frame
$\bar{\tau}^B$	Total external moment vector applied to the body about its center of mass expressed in the body frame
\bar{f}^B	Total external force vector applied to the body expressed in the body frame
1	Dual quaternion $1 + \epsilon 0$
0	Dual quaternion $0 + \epsilon 0$
$q_{Y/Z}$	Unit dual quaternion from the Z-frame to the Y-frame
$\omega_{Y/Z}^X$	Dual velocity of the Y-frame with respect to the Z-frame expressed in the X-frame
f^B	Total external dual force applied to the body about its center of mass expressed in the body frame
M^B	Dual inertia matrix
f_c^B	Dual control force expressed in the body frame

1. INTRODUCTION

The term “proximity operations” has been widely used in recent years to describe a wide range of space missions that require a spacecraft to remain close to another space object. Such missions can include the inspection, health monitoring, surveillance, servicing, and refueling of a space asset by another spacecraft. One of the biggest challenges in autonomous space proximity operations, either cooperative or uncooperative, is the need to autonomously and accurately track time-varying relative position and attitude references—i.e., pose references—with respect to a moving target, in order to avoid on-orbit collisions and achieve the overall mission goals. In addition, if the target spacecraft is uncooperative, the guidance, navigation, and control system of the chaser spacecraft must not rely on any help from the target spacecraft. In this case, vision-based sensors, such as cameras, are typically used to measure the relative pose between the spacecraft. Although vision-based sensors have several attractive properties, they introduce new challenges, such as a lack of direct linear- and angular-velocity measurements.

Velocity-free pose-tracking controllers have been proposed by several authors. In particular, a velocity-free

pose-tracking controller that does not require mass and inertia matrix information is proposed in [1]. However, as explained in [2], if the reference pose is not sufficiently exciting, the pose of the body might not converge to the desired pose. In [3], another velocity-free pose-tracking controller is designed based on the vectrix formalism. This controller suffers from two problems. First, the attitude of the body cannot be more than 180° away from the desired attitude. Second, the region of convergence is dependent on the gains chosen by the user. In other words, an arbitrarily large region of convergence requires arbitrarily large gains. In turn, high gains may lead to actuator saturation and poor noise rejection. Finally, in [4], it is shown that a locally asymptotically stable closed-loop system can be obtained by combining an almost globally asymptotically stable attitude-only tracking controller with a locally exponentially convergent angular-velocity observer. Although the theory presented in [4] can, in principle, be extended to pose control, only attitude control is demonstrated.

Compared to the existing literature, the velocity-free pose-tracking controller presented in this paper is almost globally asymptotically stable. In particular, the pose of the body converges to the desired pose independently of the initial condition, and unlike in [1], the reference motion does not need to be exciting. Moreover, the region of convergence does not depend on the gains chosen by the user. Note that “almost-global” stability means stability for all initial conditions, except for a set of measure 0 as a result of topological obstructions [5]. In that sense, almost-global stability is the strongest type of stability one can hope for using continuous controllers for this system.

As in the recent papers [6–8], the analogies between quaternions and dual quaternions are explored to develop the controller proposed in this paper. Dual quaternions are built on, and are an extension of, classical quaternions. They provide a compact representation of not only the attitude but also the position of a frame with respect to another frame. Their properties, including examples of previous applications, are discussed in length in [7]. However, the property that makes dual quaternions most appealing is that the combined translational and rotational kinematic and dynamic equations of motion written in terms of dual quaternions have the same form as the rotational-only kinematic and dynamic equations of motion written in terms of quaternions (albeit the operations have now to be interpreted in dual-quaternion algebra). As a consequence, as shown in [6, 7], pose controllers with certain properties can be developed from existing attitude-only controllers with analogous properties by (almost) just replacing quaternions with dual quaternions. Following the same idea, a velocity-free pose-tracking controller is developed in this paper based on the attitude-tracking controller of [9] that guarantees almost globally asymptotic stability of the attitude-tracking error when angular-velocity measurements are not available.

This paper is organized as follows. In Section II, the main operations and properties of quaternions and dual quaternions are reviewed. Then a pose-tracking controller that requires relative linear- and angular-velocity measurements is derived in Section III. Based on this velocity-feedback controller, the velocity-free controller is derived in Section IV. Subsequently, both controllers are verified numerically in Section V. Two examples are presented. In the first, a chaser spacecraft is required to track an elliptical motion around a target satellite while pointing at it. In the second, the velocity-free controller is compared qualitatively and quantitatively to the velocity-feedback controller fed with velocity estimates produced by an extended Kalman filter (EKF) through a more realistic satellite proximity-operation simulation.

II. MATHEMATICAL PRELIMINARIES

For the benefit of the reader, the main properties of quaternions and dual quaternions are summarized in this section. For additional information, the reader is referred to [7, 8, 10].

A. Quaternions

A quaternion can be represented as an ordered pair $q = (q_0, \bar{q})$, where $\bar{q} = [q_1 \ q_2 \ q_3]^T \in \mathbb{R}^3$ is the vector part of the quaternion and $q_0 \in \mathbb{R}$ is the scalar part. Henceforth, quaternions with zero scalar part and with zero vector part will be referred to, respectively, as vector quaternions and scalar quaternions. The sets of quaternions, vector quaternions, and scalar quaternions will be respectively denoted by $\mathbb{H} = \{q : q = (q_0, \bar{q}), \bar{q} \in \mathbb{R}^3, q_0 \in \mathbb{R}\}$, $\mathbb{H}^v = \{q \in \mathbb{H} : q_0 = 0\}$, and $\mathbb{H}^s = \{q \in \mathbb{H} : \bar{q} = 0_{3 \times 1}\}$. The following are the elementary operations on quaternions:

$$\text{Addition: } a + b = (a_0 + b_0, \bar{a} + \bar{b}) \in \mathbb{H}$$

$$\text{Multiplication by a scalar: } \lambda a = (\lambda a_0, \lambda \bar{a}) \in \mathbb{H}$$

$$\text{Multiplication: } ab = (a_0 b_0 - \bar{a} \cdot \bar{b}, a_0 \bar{b} + b_0 \bar{a} + \bar{a} \times \bar{b}) \in \mathbb{H}$$

$$\text{Conjugation: } a^* = (a_0, -\bar{a}) \in \mathbb{H}$$

$$\text{Dot product: } a \cdot b = (a_0 b_0 + \bar{a} \cdot \bar{b}, 0_{3 \times 1}) \in \mathbb{H}^s$$

$$\text{Cross product: } a \times b = (0, b_0 \bar{a} + a_0 \bar{b} + \bar{a} \times \bar{b}) \in \mathbb{H}^v$$

$$\text{Norm: } \|a\|^2 = aa^* = a^* a = a \cdot a = (a_0^2 + \bar{a} \cdot \bar{a}, 0_{3 \times 1}) \in \mathbb{H}^s$$

$$\text{Scalar part: } \text{sc}(a) = (a_0, 0_{3 \times 1}) \in \mathbb{H}^s$$

$$\text{Vector part: } \text{vec}(a) = (0, \bar{a}) \in \mathbb{H}^v$$

Multiplication by a matrix:

$$M * a = (M_{11}a_0 + M_{12}\bar{a}, M_{21}a_0 + M_{22}\bar{a}) \in \mathbb{H}.$$

In these operations, $a, b \in \mathbb{H}$, $\lambda \in \mathbb{R}$, $0_{m \times n}$ is an $m \times n$ matrix of 0s,

$$M = \begin{bmatrix} M_{11} & M_{12} \\ M_{21} & M_{22} \end{bmatrix} \in \mathbb{R}^{4 \times 4},$$

$M_{11} \in \mathbb{R}$, $M_{12} \in \mathbb{R}^{1 \times 3}$, $M_{21} \in \mathbb{R}^{3 \times 1}$, and $M_{22} \in \mathbb{R}^{3 \times 3}$.

Note that, in general, $ab \neq ba$. In this paper, the quaternions $(1, 0_{3 \times 1})$ and $(0, 0_{3 \times 1})$ will be denoted, respectively, by $\mathbf{1}$ and $\mathbf{0}$. The following properties follow from the previous definitions [10]: $a \cdot (bc) = b \cdot (ac^*) = c \cdot (b^*a)$, $\|ab\| = \|a\|\|b\|$, and $(M * a) \cdot b = a \cdot (M^T * b)$, where $a, b, c \in \mathbb{H}$ and $M \in \mathbb{R}^{4 \times 4}$. The \mathcal{L}_∞ -norm of a function $u : [0, \infty) \rightarrow \mathbb{H}$ is defined as $\|u\|_\infty = \sup_{t \geq 0} \|u(t)\|$. Moreover, $u \in \mathcal{L}_\infty$ if and only if $\|u\|_\infty < \infty$.

The relative orientation of a body frame with respect to an inertial frame can be represented by the unit quaternion $q_{B/I} = (\cos(\phi/2), \sin(\phi/2)\bar{n})$, where the body frame is said to be rotated with respect to the inertial frame about the unit vector \bar{n} (i.e., $\bar{n} \cdot \bar{n} = 1$) by an angle ϕ . The quaternion $q_{B/I}$ is a unit quaternion because it belongs to the set $\mathbb{H}^u = \{q \in \mathbb{H} : q \cdot q = 1\}$. The body coordinates \bar{v}^B of a vector can be calculated from the inertial coordinates \bar{v}^I of that same vector, and vice versa, through $v^B = q_{B/I}^* v^I q_{B/I}$ and $v^I = q_{B/I} v^B q_{B/I}^*$, where $v^X = (0, \bar{v}^X)$.

The rotational kinematic equations of the body frame and of a frame with some desired orientation, both with respect to the inertial frame and represented, respectively, by the unit quaternions $q_{B/I}$ and $q_{D/I}$, are given by

$$\dot{q}_{B/I} = \frac{1}{2} q_{B/I} \omega_{B/I}^B = \frac{1}{2} \omega_{B/I}^I q_{B/I}$$

and

$$\dot{q}_{D/I} = \frac{1}{2} q_{D/I} \omega_{D/I}^D = \frac{1}{2} \omega_{D/I}^I q_{D/I},$$

where $\omega_{Y/Z}^X = (0, \bar{\omega}_{Y/Z}^X)$ and $\bar{\omega}_{Y/Z}^X = [p_{Y/Z}^X \ q_{Y/Z}^X \ r_{Y/Z}^X]^T$ is the angular velocity of the Y-frame with respect to the Z-frame expressed in the X-frame. The error quaternion $q_{B/D} = q_{D/I}^* q_{B/I}$ is the unit quaternion that rotates the desired frame onto the body frame. Through differentiating $q_{B/D}$, the kinematic equations of the error quaternion turn out to be

$$\dot{q}_{B/D} = \frac{1}{2} q_{B/D} \omega_{B/D}^B = \frac{1}{2} \omega_{B/D}^D q_{B/D}, \quad (1)$$

where $\omega_{B/D}^B = \omega_{B/I}^B - \omega_{D/I}^B$ and $\omega_{B/D}^D = \omega_{B/I}^D - \omega_{D/I}^D$.

B. Dual Quaternions

A dual quaternion is defined as $q = q_r + \epsilon q_d$, where $q_r, q_d \in \mathbb{H}$ are the real and dual part of the dual quaternion, respectively, and ϵ is the dual unit, defined as $\epsilon^2 = 0$ and $\epsilon \neq 0$. Hereafter, dual quaternions with $q_r, q_d \in \mathbb{H}^v$ and with $q_r, q_d \in \mathbb{H}^s$ will be referred to, respectively, as dual vector quaternions and dual scalar quaternions. The sets of dual quaternions, dual scalar quaternions, and dual vector quaternions will be respectively denoted by $\mathbb{H}_d = \{q : q = q_r + \epsilon q_d, q_r, q_d \in \mathbb{H}\}$,

$\mathbb{H}_d^s = \{q : q = q_r + \epsilon q_d, q_r, q_d \in \mathbb{H}^s\}$, and $\mathbb{H}_d^v = \{q : q = q_r + \epsilon q_d, q_r, q_d \in \mathbb{H}^v\}$. Moreover, the set of dual scalar quaternions with zero dual part will be denoted by $\mathbb{H}_d^r = \{q : q = q_r + \epsilon(0, 0_{3 \times 1}), q_r \in \mathbb{H}^s\}$. The following are the elementary operations on dual quaternions:

Addition: $a + b = (a_r + b_r) + \epsilon(a_d + b_d) \in \mathbb{H}_d$

Multiplication by a scalar: $\lambda a = (\lambda a_r) + \epsilon(\lambda a_d) \in \mathbb{H}_d$

Multiplication: $ab = (a_r b_r) + \epsilon(a_r b_d + a_d b_r) \in \mathbb{H}_d$

Conjugation: $a^* = a_r^* + \epsilon a_d^* \in \mathbb{H}_d$

Swap: $a^s = a_d + \epsilon a_r \in \mathbb{H}_d$

Dot product: $a \cdot b = a_r \cdot b_r + \epsilon(a_d \cdot b_r + a_r \cdot b_d) \in \mathbb{H}_d^s$

Cross product: $a \times b = a_r \times b_r + \epsilon(a_d \times b_r + a_r \times b_d) \in \mathbb{H}_d^v$

Circle product: $a \circ b = a_r \cdot b_r + a_d \cdot b_d \in \mathbb{H}_d^r$

Dual norm: $\|a\|_d^2 = (a_r \cdot a_r) + \epsilon(2a_r \cdot a_d) \in \mathbb{H}_d^s$

Norm: $\|a\|^2 = a \circ a \in \mathbb{H}_d^r$

Scalar part: $\text{sc}(a) = \text{sc}(a_r) + \epsilon \text{sc}(a_d) \in \mathbb{H}_d^s$

Vector part: $\text{vec}(a) = \text{vec}(a_r) + \epsilon \text{vec}(a_d) \in \mathbb{H}_d^v$

Multiplication by a matrix: $M \star q = (M_{11} * q_r + M_{12} * q_d) + \epsilon(M_{21} * q_r + M_{22} * q_d) \in \mathbb{H}_d$.

In these operations, $a, b \in \mathbb{H}_d$, $\lambda \in \mathbb{R}$,

$$M = \begin{bmatrix} M_{11} & M_{12} \\ M_{21} & M_{22} \end{bmatrix},$$

and $M_{11}, M_{12}, M_{21}, M_{22} \in \mathbb{R}^{4 \times 4}$. Note that, in general, $ab \neq ba$. In this paper, the dual quaternions $\mathbf{1} + \epsilon 0$ and $\mathbf{0} + \epsilon 0$ will be denoted by $\mathbf{1}$ and $\mathbf{0}$, respectively. The following properties follow from the previous definitions [6, 10]:

$$a \circ (bc) = b^s \circ (a^s c^*) = c^s \circ (b^* a^s), \quad a, b, c \in \mathbb{H}_d \quad (2)$$

$$a \circ (b \times c) = b^s \circ (c \times a^s) = c^s \circ (a^s \times b), \quad a, b, c \in \mathbb{H}_d^v \quad (3)$$

$$a \times a = 0, \quad a \in \mathbb{H}_d^v \quad (4)$$

$$a \times b = -b \times a, \quad a, b \in \mathbb{H}_d^v \quad (5)$$

$$a^s \circ b^s = a \circ b, \quad a, b \in \mathbb{H}_d \quad (6)$$

$$\|a^s\| = \|a\|, \quad a \in \mathbb{H}_d \quad (7)$$

$$\|a^*\| = \|a\|, \quad a \in \mathbb{H}_d \quad (8)$$

$$(M \star a) \circ b = a \circ (M^T \star b), \quad a, b \in \mathbb{H}_d, \quad M \in \mathbb{R}^{8 \times 8} \quad (9)$$

$$\|\mathbf{a} \circ \mathbf{b}\| \leq \|\mathbf{a}\| \|\mathbf{b}\|, \quad \mathbf{a}, \mathbf{b} \in \mathbb{H}_d \quad (10)$$

$$\|\mathbf{a}\mathbf{b}\| \leq \sqrt{3/2} \|\mathbf{a}\| \|\mathbf{b}\|, \quad \mathbf{a}, \mathbf{b} \in \mathbb{H}_d. \quad (11)$$

The \mathcal{L}_∞ -norm of a function $\mathbf{u} : [0, \infty) \rightarrow \mathbb{H}_d$ is defined as $\|\mathbf{u}\|_\infty = \sup_{t \geq 0} \|\mathbf{u}(t)\|$. Moreover, $\mathbf{u} \in \mathcal{L}_\infty$ if and only if $\|\mathbf{u}\|_\infty < \infty$.

A compact way to represent the pose of a body frame with respect to an inertial frame is through the unit dual quaternion

$$\mathbf{q}_{B/I} = q_{B/I} + \epsilon \frac{1}{2} r_{B/I}^I q_{B/I} = q_{B/I} + \epsilon \frac{1}{2} q_{B/I} r_{B/I}^B,$$

where $\bar{r}_{Y/Z}^X = [x_{Y/Z}^X \ y_{Y/Z}^X \ z_{Y/Z}^X]^T$ and $\bar{r}_{Y/Z}^X$ is the translation vector from the origin of the Z-frame to the origin of the Y-frame expressed in the X-frame. The dual quaternion $\mathbf{q}_{B/I}$ is a unit dual quaternion because it belongs to the set

$$\mathbb{H}_d^1 = \{\mathbf{q} \in \mathbb{H}_d : \mathbf{q} \cdot \mathbf{q} = \mathbf{q}\mathbf{q}^* = \mathbf{q}^*\mathbf{q} = \|\mathbf{q}\|_d = 1\}.$$

The rotational and translational kinematic equations of the body frame and of a frame with some desired pose, both with respect to the inertial frame and represented, respectively, by the unit dual quaternions $\mathbf{q}_{B/I}$ and

$$\mathbf{q}_{D/I} = q_{D/I} + \epsilon \frac{1}{2} r_{D/I}^I q_{D/I} = q_{D/I} + \epsilon \frac{1}{2} q_{D/I} r_{D/I}^D,$$

are given by

$$\dot{\mathbf{q}}_{B/I} = \frac{1}{2} \boldsymbol{\omega}_{B/I}^I \mathbf{q}_{B/I} = \frac{1}{2} \mathbf{q}_{B/I} \boldsymbol{\omega}_{B/I}^B$$

and

$$\dot{\mathbf{q}}_{D/I} = \frac{1}{2} \boldsymbol{\omega}_{D/I}^I \mathbf{q}_{D/I} = \frac{1}{2} \mathbf{q}_{D/I} \boldsymbol{\omega}_{D/I}^D,$$

where $\boldsymbol{\omega}_{Y/Z}^X$ is the dual velocity of the Y-frame with respect to the Z-frame expressed in the X-frame, $\boldsymbol{\omega}_{Y/Z}^X = \boldsymbol{\omega}_{Y/Z}^X + \epsilon(v_{Y/Z}^X + \boldsymbol{\omega}_{Y/Z}^X \times r_{X/Y}^X)$, $v_{Y/Z}^X = (0, \bar{v}_{Y/Z}^X)$, and $\bar{v}_{Y/Z}^X = [u_{Y/Z}^X \ v_{Y/Z}^X \ w_{Y/Z}^X]^T$ is the linear velocity of the origin of the Y-frame with respect to the Z-frame expressed in the X-frame.

By direct analogy to the error quaternion, the dual error quaternion is defined as

$$\begin{aligned} \mathbf{q}_{B/D} &= \mathbf{q}_{D/I}^* \mathbf{q}_{B/I} \\ &= q_{B/D} + \epsilon \frac{1}{2} q_{B/D} r_{B/D}^B = q_{B/D} + \epsilon \frac{1}{2} r_{B/D}^D q_{B/D}. \end{aligned}$$

The dual error quaternion is the unit dual quaternion that represents the pose of the body frame with respect to the desired frame. Through differentiating $\mathbf{q}_{B/D}$, the kinematic equations of the dual error quaternion turn out to be

$$\dot{\mathbf{q}}_{B/D} = \frac{1}{2} \mathbf{q}_{B/D} \boldsymbol{\omega}_{B/D}^B = \frac{1}{2} \boldsymbol{\omega}_{B/D}^D \mathbf{q}_{B/D}, \quad (12)$$

where $\boldsymbol{\omega}_{B/D}^B = \boldsymbol{\omega}_{B/I}^B - \boldsymbol{\omega}_{D/I}^B$, $\boldsymbol{\omega}_{D/I}^B = \mathbf{q}_{B/I}^* \boldsymbol{\omega}_{D/I}^D \mathbf{q}_{B/I}$, and $\boldsymbol{\omega}_{B/I}^D = \mathbf{q}_{B/D} \boldsymbol{\omega}_{B/I}^B \mathbf{q}_{B/D}^*$. Note that (12) has the same form as (1).

The dual-quaternion representation of the relative rotational and translational dynamic equations of a rigid

body are given by

$$\begin{aligned} (\dot{\boldsymbol{\omega}}_{B/D}^B)^s &= (M^B)^{-1} \star (\mathbf{f}^B - (\boldsymbol{\omega}_{B/D}^B + \boldsymbol{\omega}_{D/I}^B) \\ &\quad \times (M^B \star ((\boldsymbol{\omega}_{B/D}^B)^s + (\boldsymbol{\omega}_{D/I}^B)^s)) \\ &\quad - M^B \star (\mathbf{q}_{B/D}^* \dot{\boldsymbol{\omega}}_{D/I}^D \mathbf{q}_{B/D})^s \\ &\quad - M^B \star (\boldsymbol{\omega}_{D/I}^B \times \boldsymbol{\omega}_{B/D}^B)^s), \end{aligned} \quad (13)$$

where $\mathbf{f}^B = \mathbf{f}^B + \epsilon \boldsymbol{\tau}^B$ is the total external dual force applied to the body about its center of mass expressed in the body frame, $\mathbf{f}^B = (0, \bar{f}^B)$, $\bar{f}^B = [f_1^B \ f_2^B \ f_3^B]^T$ is the total external force vector applied to the body expressed in the body frame, $\boldsymbol{\tau}^B = (0, \bar{\tau}^B)$, and $\bar{\tau}^B = [\tau_1^B \ \tau_2^B \ \tau_3^B]^T$ is the total external moment vector applied to the body about its center of mass expressed in the body frame. Finally, $M^B \in \mathbb{R}^{8 \times 8}$ is the dual inertia matrix, defined as

$$M^B = \begin{bmatrix} 1 & \mathbf{0}_{1 \times 3} & 0 & \mathbf{0}_{1 \times 3} \\ \mathbf{0}_{3 \times 1} & m \mathbf{I}_{3 \times 3} & \mathbf{0}_{3 \times 1} & \mathbf{0}_{3 \times 3} \\ 0 & \mathbf{0}_{1 \times 3} & 1 & \mathbf{0}_{1 \times 3} \\ \mathbf{0}_{3 \times 1} & \mathbf{0}_{3 \times 3} & \mathbf{0}_{3 \times 1} & \bar{I}^B \end{bmatrix};$$

$$I^B = \begin{bmatrix} 1 & \mathbf{0}_{1 \times 3} \\ \mathbf{0}_{3 \times 1} & \bar{I}^B \end{bmatrix};$$

$\bar{I}^B \in \mathbb{R}^{3 \times 3}$ is the mass moment of inertia of the body about its center of mass written in the body frame; and m is the mass of the body. Note that M^B is a symmetric positive-definite matrix. Also note the similarity between (13) and the quaternion representation of the relative rotational(-only) dynamic equations given by $\dot{\boldsymbol{\omega}}_{B/D}^B = (I^B)^{-1} \star (\boldsymbol{\tau}^B - (\boldsymbol{\omega}_{B/D}^B + \boldsymbol{\omega}_{D/I}^B) \times (I^B \star (\boldsymbol{\omega}_{B/D}^B + \boldsymbol{\omega}_{D/I}^B)) - I^B \star (\mathbf{q}_{B/D}^* \dot{\boldsymbol{\omega}}_{D/I}^D \mathbf{q}_{B/D}) - I^B \star (\boldsymbol{\omega}_{D/I}^B \times \boldsymbol{\omega}_{B/D}^B))$.

III. VELOCITY-FEEDBACK POSE-TRACKING CONTROLLER

When the relative linear and angular velocities are known, the controller proposed in Theorem 1 can be used to track a time-varying reference pose.

THEOREM 1 Consider the rigid-body relative kinematic and dynamic equations (12) and (13). Let the total external dual force acting on the rigid body be defined by the feedback control law

$$\begin{aligned} \mathbf{f}^B &= -k_p \text{vec}(\mathbf{q}_{B/D}^* (\mathbf{q}_{B/D}^s - \mathbf{1}^s)) - k_d (\boldsymbol{\omega}_{B/D}^B)^s \\ &\quad + M^B \star (\mathbf{q}_{B/D}^* \dot{\boldsymbol{\omega}}_{D/I}^D \mathbf{q}_{B/D})^s + \boldsymbol{\omega}_{D/I}^B \times (M^B \star (\boldsymbol{\omega}_{D/I}^B)^s), \end{aligned} \quad (14)$$

$k_p, k_d > 0$, and assume that $\boldsymbol{\omega}_{D/I}^D, \boldsymbol{\omega}_{D/I}^B \in \mathcal{L}_\infty$. Then $\mathbf{q}_{B/D} \rightarrow \pm \mathbf{1}$ (i.e., $q_{B/D} \rightarrow \pm 1$ and $r_{B/D}^B \rightarrow 0$) and $\boldsymbol{\omega}_{B/D}^B \rightarrow \mathbf{0}$ (i.e., $\boldsymbol{\omega}_{B/D}^B \rightarrow 0$ and $v_{B/D}^B \rightarrow 0$) as $t \rightarrow +\infty$ for all initial conditions.

PROOF First, note that $\mathbf{q}_{B/D} = \pm \mathbf{1}$ and $\boldsymbol{\omega}_{B/D}^B = \mathbf{0}$ are in fact the equilibrium conditions for the closed-loop system

formed by (12)–(14). Consider now the following candidate Lyapunov function for the equilibrium point $\mathbf{q}_{B/D} = +\mathbf{1}$ and $\boldsymbol{\omega}_{B/D}^B = \mathbf{0}$ —or, equivalently, $(\boldsymbol{\omega}_{B/D}^B)^s = \mathbf{0}$:

$$V(\mathbf{q}_{B/D}, \boldsymbol{\omega}_{B/D}^B) = k_p(\mathbf{q}_{B/D} - \mathbf{1}) \circ (\mathbf{q}_{B/D} - \mathbf{1}) + \frac{1}{2}(\boldsymbol{\omega}_{B/D}^B)^s \circ (M^B \star (\boldsymbol{\omega}_{B/D}^B)^s).$$

Note that V is a valid candidate Lyapunov function, since $V(\mathbf{q}_{B/D} = \mathbf{1}, \boldsymbol{\omega}_{B/D}^B = \mathbf{0}) = 0$ and $V(\mathbf{q}_{B/D}, \boldsymbol{\omega}_{B/D}^B) > 0$ for all $(\mathbf{q}_{B/D}, \boldsymbol{\omega}_{B/D}^B) \in \mathbb{H}_d^u \times \mathbb{H}_d^v \setminus \{\mathbf{1}, \mathbf{0}\}$. The time derivative of V is equal to $\dot{V} = 2k_p(\mathbf{q}_{B/D} - \mathbf{1}) \circ \dot{\mathbf{q}}_{B/D} + (\boldsymbol{\omega}_{B/D}^B)^s \circ (M^B \star (\dot{\boldsymbol{\omega}}_{B/D}^B)^s)$. Then, plugging in (12) and (13) and using (3), it follows that $\dot{V} = (\boldsymbol{\omega}_{B/D}^B)^s \circ (k_p \mathbf{q}_{B/D}^* (\mathbf{q}_{B/D}^s - \mathbf{1})^s + \mathbf{f}^B - (\boldsymbol{\omega}_{B/D}^B + \boldsymbol{\omega}_{D/I}^B) \times (M^B \star ((\boldsymbol{\omega}_{B/D}^B)^s + (\boldsymbol{\omega}_{D/I}^B)^s)) - M^B \star (\mathbf{q}_{B/D}^* \dot{\boldsymbol{\omega}}_{D/I}^D \mathbf{q}_{B/D})^s - M^B \star (\boldsymbol{\omega}_{D/I}^B \times \boldsymbol{\omega}_{B/D}^B)^s)$. Introducing the feedback control law (14) yields $\dot{V} = (\boldsymbol{\omega}_{B/D}^B)^s \circ (-k_d(\boldsymbol{\omega}_{B/D}^B)^s) + (\boldsymbol{\omega}_{B/D}^B)^s \circ (k_p \mathbf{q}_{B/D}^* (\mathbf{q}_{B/D}^s - \mathbf{1})^s - k_p \text{vec}(\mathbf{q}_{B/D}^* (\mathbf{q}_{B/D}^s - \mathbf{1})^s)) + (\boldsymbol{\omega}_{B/D}^B)^s \circ (-(\boldsymbol{\omega}_{B/D}^B + \boldsymbol{\omega}_{D/I}^B) \times (M^B \star ((\boldsymbol{\omega}_{B/D}^B)^s + (\boldsymbol{\omega}_{D/I}^B)^s)) - M^B \star (\boldsymbol{\omega}_{D/I}^B \times \boldsymbol{\omega}_{B/D}^B)^s + \boldsymbol{\omega}_{D/I}^B \times (M^B \star (\boldsymbol{\omega}_{D/I}^B)^s))$. Note that the second term is zero because it is the circle product of a dual vector quaternion with a dual scalar quaternion. Moreover, the third term can be shown to be equal to zero as follows:

$$\begin{aligned} & (\boldsymbol{\omega}_{B/D}^B)^s \circ \left(-(\boldsymbol{\omega}_{B/D}^B + \boldsymbol{\omega}_{D/I}^B) \times \left(M^B \star \left((\boldsymbol{\omega}_{B/D}^B)^s + (\boldsymbol{\omega}_{D/I}^B)^s \right) \right) - M^B \star (\boldsymbol{\omega}_{D/I}^B \times \boldsymbol{\omega}_{B/D}^B)^s + \boldsymbol{\omega}_{D/I}^B \times \left(M^B \star (\boldsymbol{\omega}_{D/I}^B)^s \right) \right) \\ &= \left((\boldsymbol{\omega}_{B/D}^B)^s - (\boldsymbol{\omega}_{D/I}^B)^s \right) \circ \left(-\boldsymbol{\omega}_{B/D}^B \times \left(M^B \star (\boldsymbol{\omega}_{B/D}^B)^s \right) - M^B \star (\boldsymbol{\omega}_{D/I}^B \times (\boldsymbol{\omega}_{B/D}^B - \boldsymbol{\omega}_{D/I}^B))^s + \boldsymbol{\omega}_{D/I}^B \times \left(M^B \star (\boldsymbol{\omega}_{D/I}^B)^s \right) \right) \\ &= (\boldsymbol{\omega}_{B/D}^B)^s \circ \left(-\boldsymbol{\omega}_{B/D}^B \times \left(M^B \star (\boldsymbol{\omega}_{B/D}^B)^s \right) - M^B \star (\boldsymbol{\omega}_{D/I}^B \times \boldsymbol{\omega}_{B/D}^B)^s + \boldsymbol{\omega}_{D/I}^B \times \left(M^B \star (\boldsymbol{\omega}_{D/I}^B)^s \right) \right) - (\boldsymbol{\omega}_{D/I}^B)^s \\ &\quad \circ \left(-\boldsymbol{\omega}_{B/D}^B \times \left(M^B \star (\boldsymbol{\omega}_{B/D}^B)^s \right) - M^B \star (\boldsymbol{\omega}_{D/I}^B \times \boldsymbol{\omega}_{B/D}^B)^s + \boldsymbol{\omega}_{D/I}^B \times \left(M^B \star (\boldsymbol{\omega}_{D/I}^B)^s \right) \right) \\ &= -(\boldsymbol{\omega}_{B/D}^B)^s \circ \left(\boldsymbol{\omega}_{B/D}^B \times \left(M^B \star (\boldsymbol{\omega}_{B/D}^B)^s \right) \right) - (\boldsymbol{\omega}_{B/D}^B)^s \circ \left(M^B \star (\boldsymbol{\omega}_{D/I}^B \times \boldsymbol{\omega}_{B/D}^B)^s \right) + (\boldsymbol{\omega}_{B/D}^B)^s \\ &\quad \circ \left(\boldsymbol{\omega}_{D/I}^B \times \left(M^B \star (\boldsymbol{\omega}_{D/I}^B)^s \right) \right) + (\boldsymbol{\omega}_{D/I}^B)^s \circ \left(\boldsymbol{\omega}_{B/D}^B \times \left(M^B \star (\boldsymbol{\omega}_{B/D}^B)^s \right) \right) + (\boldsymbol{\omega}_{D/I}^B)^s \circ \left(M^B \star (\boldsymbol{\omega}_{D/I}^B \times \boldsymbol{\omega}_{B/D}^B)^s \right) \\ &\quad - (\boldsymbol{\omega}_{D/I}^B)^s \circ \left(\boldsymbol{\omega}_{D/I}^B \times \left(M^B \star (\boldsymbol{\omega}_{D/I}^B)^s \right) \right). \end{aligned}$$

Note that the first and last terms are zero due to (3) and (4). Moreover, using (6) and (9), the second and fifth terms can be rewritten as $-(M^B \star (\boldsymbol{\omega}_{B/D}^B)^s)^s \circ (\boldsymbol{\omega}_{D/I}^B \times \boldsymbol{\omega}_{B/D}^B)^s + (\boldsymbol{\omega}_{B/D}^B)^s \circ (\boldsymbol{\omega}_{D/I}^B \times (M^B \star (\boldsymbol{\omega}_{D/I}^B)^s)) + (\boldsymbol{\omega}_{D/I}^B)^s \circ (\boldsymbol{\omega}_{B/D}^B \times (M^B \star (\boldsymbol{\omega}_{B/D}^B)^s)) + (M^B \star (\boldsymbol{\omega}_{D/I}^B)^s)^s \circ (\boldsymbol{\omega}_{D/I}^B \times \boldsymbol{\omega}_{B/D}^B)$. Finally, applying (3) and (5) to the first and last terms of the previous expression yields $-(\boldsymbol{\omega}_{D/I}^B)^s \circ (\boldsymbol{\omega}_{B/D}^B \times (M^B \star (\boldsymbol{\omega}_{B/D}^B)^s)) + (\boldsymbol{\omega}_{B/D}^B)^s \circ (\boldsymbol{\omega}_{D/I}^B \times (M^B \star (\boldsymbol{\omega}_{D/I}^B)^s)) + (\boldsymbol{\omega}_{D/I}^B)^s \circ (\boldsymbol{\omega}_{B/D}^B \times (M^B \star (\boldsymbol{\omega}_{B/D}^B)^s)) - (\boldsymbol{\omega}_{B/D}^B)^s \circ (\boldsymbol{\omega}_{D/I}^B \times (M^B \star (\boldsymbol{\omega}_{D/I}^B)^s)) = \mathbf{0}$. Therefore, the time

derivative of the Lyapunov function is equal to

$$\dot{V} = -k_d(\boldsymbol{\omega}_{B/D}^B)^s \circ (\boldsymbol{\omega}_{B/D}^B)^s \leq 0 \text{ for all}$$

$(\mathbf{q}_{B/D}, \boldsymbol{\omega}_{B/D}^B) \in \mathbb{H}_d^u \times \mathbb{H}_d^v \setminus \{\mathbf{1}, \mathbf{0}\}$. Hence, $\mathbf{q}_{B/D}$ and $\boldsymbol{\omega}_{B/D}^B$ are uniformly bounded—i.e., $\mathbf{q}_{B/D}, \boldsymbol{\omega}_{B/D}^B \in \mathcal{L}_\infty$.

Since $V \geq 0$ and $\dot{V} \leq 0$, $\lim_{t \rightarrow \infty} V(t)$ exists and is finite. By integrating both sides of

$$\dot{V} = -k_d(\boldsymbol{\omega}_{B/D}^B)^s \circ (\boldsymbol{\omega}_{B/D}^B)^s \leq 0, \text{ one obtains}$$

$$\lim_{t \rightarrow \infty} \int_0^t \dot{V}(\tau) d\tau = \lim_{t \rightarrow \infty} V(t) - V(0) \leq -\lim_{t \rightarrow \infty} \int_0^t k_d(\boldsymbol{\omega}_{B/D}^B(\tau))^s \circ (\boldsymbol{\omega}_{B/D}^B(\tau))^s d\tau \text{ or}$$

$$\lim_{t \rightarrow \infty} \int_0^t k_d(\boldsymbol{\omega}_{B/D}^B(\tau))^s \circ (\boldsymbol{\omega}_{B/D}^B(\tau))^s d\tau \leq V(0). \quad (15)$$

Since $\mathbf{q}_{B/D}, \boldsymbol{\omega}_{B/D}^B \in \mathcal{L}_\infty$ and $\dot{\boldsymbol{\omega}}_{D/I}^D, \boldsymbol{\omega}_{D/I}^B \in \mathcal{L}_\infty$ by assumption, it follows from (14) that $\mathbf{f}^B \in \mathcal{L}_\infty$ as well. Then from (13) it also follows that $\dot{\boldsymbol{\omega}}_{B/D}^B \in \mathcal{L}_\infty$. Along with (15), this implies that $\boldsymbol{\omega}_{B/D}^B(t) \rightarrow \mathbf{0}$ as $t \rightarrow \infty$, according to Barbalat's lemma [11].

It can also be shown that $\dot{\boldsymbol{\omega}}_{B/D}^B \rightarrow \mathbf{0}$ as $t \rightarrow \infty$. First, note that $\lim_{t \rightarrow \infty} \int_0^t \dot{\boldsymbol{\omega}}_{B/D}^B(\tau) d\tau = \lim_{t \rightarrow \infty} \boldsymbol{\omega}_{B/D}^B(t) - \boldsymbol{\omega}_{B/D}^B(0) = -\boldsymbol{\omega}_{B/D}^B(0)$ exists and is finite. Now note that $\ddot{\boldsymbol{\omega}}_{B/D}^B \in \mathcal{L}_\infty$, since $\dot{\boldsymbol{\omega}}_{D/I}^D, \boldsymbol{\omega}_{D/I}^B, \dot{\boldsymbol{\omega}}_{B/D}^B, \boldsymbol{\omega}_{B/D}^B, \mathbf{q}_{B/D}, \dot{\mathbf{q}}_{B/D} \in \mathcal{L}_\infty$. Hence, by Barbalat's lemma, $\dot{\boldsymbol{\omega}}_{B/D}^B \rightarrow \mathbf{0}$ as $t \rightarrow \infty$.

Finally, calculating the limit as $t \rightarrow \infty$ of both sides of (13) yields $\text{vec}(\mathbf{q}_{B/D}^* (\mathbf{q}_{B/D}^s - \mathbf{1})^s) \rightarrow \mathbf{0}$ as $t \rightarrow \infty$, which, as shown in [12], is equivalent to $\mathbf{q}_{B/D} \rightarrow \pm \mathbf{1}$.

REMARK 1 The dual part of control law (14) is

$$\tau^B = -k_p \text{vec}(\mathbf{q}_{B/D}) - k_d \boldsymbol{\omega}_{B/D}^B + I^B * (\mathbf{q}_{B/D}^* \dot{\boldsymbol{\omega}}_{D/I}^D \mathbf{q}_{B/D}) + \boldsymbol{\omega}_{D/I}^B \times (I^B * \boldsymbol{\omega}_{D/I}^B). \text{ This control law is identical to the attitude(-only) model-dependent control law proposed in [13].}$$

IV. VELOCITY-FREE POSE-TRACKING CONTROLLER

The pose-tracking controller presented in Section III is almost globally asymptotically stable, but it requires measurements of $\boldsymbol{\omega}_{B/D}^B$. Theorem 2 shows that it is still possible to obtain an almost globally asymptotically stable pose-tracking controller without measurements of $\boldsymbol{\omega}_{B/D}^B$.

THEOREM 2 Consider the rigid-body relative kinematic and dynamic equations (12) and (13). Let the total external dual force acting on the rigid body be defined by the feedback control law

$$\begin{aligned} \mathbf{f}^B &= -k_p \text{vec}(\mathbf{q}_{B/D}^* (\mathbf{q}_{B/D}^s - \mathbf{1}^s)) - 2 \text{vec}(\mathbf{q}_{B/D}^* \mathbf{z}^s) \\ &\quad + M^B \star (\mathbf{q}_{B/D}^* \dot{\omega}_{D/I}^D \mathbf{q}_{B/D})^s + \omega_{D/I}^B \times (M^B \star (\omega_{D/I}^B)^s), \\ k_p &> 0, \end{aligned} \quad (16)$$

where \mathbf{z} is the output of the linear time-invariant (LTI) system

$$\dot{\mathbf{x}}_p = A \star \mathbf{x}_p + B \star \mathbf{q}_{B/D} \text{ and } \mathbf{z} = (CA) \star \mathbf{x}_p + (CB) \star \mathbf{q}_{B/D}, \quad (17)$$

(A, B, C) is a minimal realization of a strictly positive real transfer matrix $C_{sp}(s)$, and B is a full-rank matrix. Assume that $\dot{\omega}_{D/I}^D, \omega_{D/I}^D \in \mathcal{L}_\infty$. Then $\mathbf{q}_{B/D} \rightarrow \pm \mathbf{1}$, $\omega_{B/D}^B \rightarrow \mathbf{0}$, and $\mathbf{x}_{sp} = \dot{\mathbf{x}}_p \rightarrow \mathbf{0}$ as $t \rightarrow +\infty$ for all initial conditions.

PROOF First, rewrite the LTI system as

$$\dot{\mathbf{x}}_{sp} = A \star \mathbf{x}_{sp} + B \star \dot{\mathbf{q}}_{B/D} \text{ and } \mathbf{z} = C \star \mathbf{x}_{sp}. \quad (18)$$

Note that $\mathbf{q}_{B/D} = \pm \mathbf{1}$, $\omega_{B/D}^B = \mathbf{0}$, and $\mathbf{x}_{sp} = \mathbf{0}$ is the equilibrium condition of the closed-loop system formed by (12), (13), (16), and (18). Consider the candidate Lyapunov function

$$\begin{aligned} V(\mathbf{q}_{B/D}, \omega_{B/D}^B, \mathbf{x}_{sp}) &= k_p (\mathbf{q}_{B/D} - \mathbf{1}) \circ (\mathbf{q}_{B/D} - \mathbf{1}) \\ &\quad + \frac{1}{2} (\omega_{B/D}^B)^s \circ (M^B \star (\omega_{B/D}^B)^s) \\ &\quad + 2 \mathbf{x}_{sp} \circ (P \star \mathbf{x}_{sp}), \end{aligned}$$

for the equilibrium point $\mathbf{q}_{B/D} = \mathbf{1}$, $\omega_{B/D}^B = \mathbf{0}$, $\mathbf{x}_{sp} = \mathbf{0}$, where $P = P^T > 0$ satisfies $A^T P + P A = -Q$, $P B = C^T$, and $Q = Q^T > 0$. By the Kalman–Yakubovich–Popov conditions [11], there always exist matrices P and Q satisfying these conditions, since (A, B, C) is a minimal realization of a strictly positive real transfer matrix $C_{sp}(s)$. Note that V is a valid candidate Lyapunov function, since $V(\mathbf{q}_{B/D} = \mathbf{1}, \omega_{B/D}^B = \mathbf{0}, \mathbf{x}_{sp} = \mathbf{0}) = 0$ and $V(\mathbf{q}_{B/D}, \omega_{B/D}^B, \mathbf{x}_{sp}) > 0$ for all $(\mathbf{q}_{B/D}, \omega_{B/D}^B, \mathbf{x}_{sp}) \in \mathbb{H}_d^u \times \mathbb{H}_d^v \times \mathbb{H}_d \setminus \{\mathbf{1}, \mathbf{0}, \mathbf{0}\}$. The time derivative of V is equal to $\dot{V} = 2k_p (\mathbf{q}_{B/D} - \mathbf{1}) \circ \dot{\mathbf{q}}_{B/D} + (\omega_{B/D}^B)^s \circ (M^B \star (\dot{\omega}_{B/D}^B)^s) + 4 \dot{\mathbf{x}}_{sp} \circ (P \star \mathbf{x}_{sp})$. From plugging in (12) and (13) and applying (2) and the Kalman–Yakubovich–Popov conditions, it follows that $\dot{V} = (\omega_{B/D}^B)^s \circ (k_p \mathbf{q}_{B/D}^* (\mathbf{q}_{B/D}^s - \mathbf{1}^s) + \mathbf{f}^B - (\omega_{B/D}^B + \omega_{D/I}^B) \times (M^B \star ((\omega_{B/D}^B)^s + (\omega_{D/I}^B)^s)) - M^B \star (\mathbf{q}_{B/D}^* \dot{\omega}_{D/I}^D \mathbf{q}_{B/D})^s - M^B \star (\omega_{D/I}^B \times \omega_{B/D}^B)^s) + 4(A \star \mathbf{x}_{sp} + B \star \dot{\mathbf{q}}_{B/D}) \circ (P \star \mathbf{x}_{sp})$. Introducing the feedback control law (16) yields $\dot{V} = (\omega_{B/D}^B)^s \circ (-2 \text{vec}(\mathbf{q}_{B/D}^* \mathbf{z}^s)) + (\omega_{B/D}^B)^s \circ (k_p \mathbf{q}_{B/D}^* (\mathbf{q}_{B/D}^s - \mathbf{1}^s) - k_p \text{vec}(\mathbf{q}_{B/D}^* (\mathbf{q}_{B/D}^s - \mathbf{1}^s))) + (\omega_{B/D}^B)^s \circ (-\omega_{B/D}^B + \omega_{D/I}^B) \times (M^B \star ((\omega_{B/D}^B)^s + (\omega_{D/I}^B)^s)) - M^B \star (\omega_{D/I}^B \times \omega_{B/D}^B)^s + \omega_{D/I}^B \times (M^B \star (\omega_{B/D}^B)^s) + 4(A \star \mathbf{x}_{sp} + B \star \dot{\mathbf{q}}_{B/D}) \circ (P \star \mathbf{x}_{sp})$. Again, note that the second term is zero because it is the circle product of a dual vector quaternion with a dual scalar quaternion.

Moreover, the third term has been shown to be equal to zero in the proof of Theorem 1.

As for the fourth term, it can be simplified as follows:

$$\begin{aligned} \dot{V} &= (\omega_{B/D}^B)^s \circ (-2 \text{vec}(\mathbf{q}_{B/D}^* \mathbf{z}^s)) + 4(A \star \mathbf{x}_{sp}) \\ &\quad \circ (P \star \mathbf{x}_{sp}) + 4(B \star \dot{\mathbf{q}}_{B/D}) \circ (P \star \mathbf{x}_{sp}) \\ &= (\omega_{B/D}^B)^s \circ (-2 \text{vec}(\mathbf{q}_{B/D}^* \mathbf{z}^s)) + 2((A^T P + P A) \star \mathbf{x}_{sp}) \\ &\quad \circ \mathbf{x}_{sp} + 4 \dot{\mathbf{q}}_{B/D} \circ ((B^T P) \star \mathbf{x}_{sp}) \\ &= (\omega_{B/D}^B)^s \circ (-2 \text{vec}(\mathbf{q}_{B/D}^* \mathbf{z}^s)) - 2 \mathbf{x}_{sp} \circ (Q \star \mathbf{x}_{sp}) \\ &\quad + 2(\mathbf{q}_{B/D} \omega_{B/D}^B) \circ (C \star \mathbf{x}_{sp}) \\ &= (\omega_{B/D}^B)^s \circ (2 \mathbf{q}_{B/D}^* \mathbf{z}^s - 2 \text{vec}(\mathbf{q}_{B/D}^* \mathbf{z}^s)) - 2 \mathbf{x}_{sp} \circ (Q \star \mathbf{x}_{sp}) \\ &= -2 \mathbf{x}_{sp} \circ (Q \star \mathbf{x}_{sp}) \leq 0 \end{aligned}$$

for all $(\mathbf{q}_{B/D}, \omega_{B/D}^B, \mathbf{x}_{sp}) \in \mathbb{H}_d^u \times \mathbb{H}_d^v \times \mathbb{H}_d \setminus \{\mathbf{1}, \mathbf{0}, \mathbf{0}\}$.

Hence, $\mathbf{q}_{B/D}$, $\omega_{B/D}^B$, and \mathbf{x}_{sp} are uniformly bounded—i.e., $\mathbf{q}_{B/D}, \omega_{B/D}^B, \mathbf{x}_{sp} \in \mathcal{L}_\infty$.

It is now shown that $\mathbf{x}_{sp} \rightarrow \mathbf{0}$ as $t \rightarrow \infty$. Since $V \geq 0$ and $\dot{V} \leq 0$, $\lim_{t \rightarrow \infty} V(t)$ exists and is finite. By integrating both sides of $\dot{V} = -2 \mathbf{x}_{sp} \circ (Q \star \mathbf{x}_{sp}) \leq 0$, one obtains $\lim_{t \rightarrow \infty} \int_0^t \dot{V}(\tau) d\tau = \lim_{t \rightarrow \infty} V(t) - V(0) = -\lim_{t \rightarrow \infty} \int_0^t 2 \mathbf{x}_{sp}(\tau) \circ (Q \star \mathbf{x}_{sp}(\tau)) d\tau$ or

$$\lim_{t \rightarrow \infty} \int_0^t 2 \mathbf{x}_{sp}(\tau) \circ (Q \star \mathbf{x}_{sp}(\tau)) d\tau \leq V(0). \quad (19)$$

Since $\mathbf{q}_{B/D}, \omega_{B/D}^B, \mathbf{x}_{sp} \in \mathcal{L}_\infty$, it follows that $\dot{\mathbf{q}}_{B/D} \in \mathcal{L}_\infty$ and $\dot{\mathbf{x}}_{sp} \in \mathcal{L}_\infty$. Along with (19), this implies that $\mathbf{x}_{sp} \rightarrow \mathbf{0}$ as $t \rightarrow \infty$, according to Barbalat's lemma. This, in turn, implies from (18) that $\mathbf{z} \rightarrow \mathbf{0}$ as $t \rightarrow \infty$.

It can also be shown that $\dot{\mathbf{x}}_{sp} \rightarrow \mathbf{0}$ as $t \rightarrow \infty$. First, note that $\lim_{t \rightarrow \infty} \int_0^t \dot{\mathbf{x}}_{sp}(\tau) d\tau = \lim_{t \rightarrow \infty} \mathbf{x}_{sp}(t) - \mathbf{x}_{sp}(0) = -\mathbf{x}_{sp}(0)$ exists and is finite. Since $\dot{\mathbf{x}}_{sp} = A \star \dot{\mathbf{x}}_{sp} + B \star \dot{\mathbf{q}}_{B/D}$ and $\mathbf{q}_{B/D}, \omega_{B/D}^B, \mathbf{x}_{sp}, \dot{\mathbf{q}}_{B/D}, \dot{\mathbf{x}}_{sp}, \dot{\omega}_{D/I}^D, \omega_{D/I}^D, \mathbf{z}, \dot{\omega}_{B/D}^B, \dot{\mathbf{q}}_{B/D} \in \mathcal{L}_\infty$, it follows that $\dot{\mathbf{x}}_{sp} \in \mathcal{L}_\infty$. Hence, by Barbalat's lemma, $\dot{\mathbf{x}}_{sp} \rightarrow \mathbf{0}$ as $t \rightarrow \infty$.

Thus, calculating the limit as $t \rightarrow \infty$ of both sides of (18) yields $\dot{\mathbf{q}}_{B/D} \rightarrow \mathbf{0}$ as $t \rightarrow \infty$, since B is assumed to be full rank. Given that (12) can be rewritten as $\omega_{B/D}^B = 2 \mathbf{q}_{B/D}^* \dot{\mathbf{q}}_{B/D}$, this also implies that $\omega_{B/D}^B \rightarrow \mathbf{0}$ as $t \rightarrow \infty$.

Now it is shown that $\dot{\omega}_{B/D}^B \rightarrow \mathbf{0}$ as $t \rightarrow \infty$. First, note that $\lim_{t \rightarrow \infty} \int_0^t \dot{\omega}_{B/D}^B(\tau) d\tau = \lim_{t \rightarrow \infty} \omega_{B/D}^B(t) - \omega_{B/D}^B(0) = -\omega_{B/D}^B(0)$ exists and is finite. Since $(\dot{\omega}_{B/D}^B)^s = (M^B)^{-1} \star (-k_p \text{vec}(\mathbf{q}_{B/D}^* (\mathbf{q}_{B/D}^s - \mathbf{1}^s)) - k_p \text{vec}(\mathbf{q}_{B/D}^* (\dot{\mathbf{q}}_{B/D}^s)) - 2 \text{vec}(\dot{\mathbf{q}}_{B/D}^* \mathbf{z}^s) - 2 \text{vec}(\mathbf{q}_{B/D}^* (\dot{\mathbf{z}}^s)) + \dot{\omega}_{D/I}^B \times (M^B \star (\omega_{D/I}^B)^s) + \omega_{D/I}^B \times (M^B \star (\dot{\omega}_{D/I}^B)^s) - \dot{\omega}_{B/I}^B \times (M^B \star (\omega_{B/I}^B)^s) - \omega_{B/I}^B \times (M^B \star (\dot{\omega}_{B/I}^B)^s) - M^B \star (\dot{\omega}_{D/I}^B \times \omega_{B/D}^B)^s - M^B \star (\omega_{D/I}^B \times \dot{\omega}_{B/D}^B)^s)$ and $\dot{\omega}_{B/D}^B, \omega_{B/D}^B, \dot{\omega}_{B/I}^B, \omega_{B/I}^B, \mathbf{q}_{B/D}, \dot{\mathbf{q}}_{B/D}, \mathbf{z}, \dot{\mathbf{z}} \in \mathcal{L}_\infty$, it follows that $\dot{\omega}_{B/D}^B \in \mathcal{L}_\infty$. Hence, by Barbalat's lemma, $\dot{\omega}_{B/D}^B \rightarrow \mathbf{0}$ as $t \rightarrow \infty$.

Finally, calculating the limit as $t \rightarrow \infty$ of both sides of (13) yields $\text{vec}(\mathbf{q}_{B/D}^* (\mathbf{q}_{B/D}^s - \mathbf{1}^s)) \rightarrow \mathbf{0}$ as $t \rightarrow \infty$, which, as shown in [12], is equivalent to $\mathbf{q}_{B/D} \rightarrow \pm \mathbf{1}$.

REMARK 2 Theorems 1 and 2 state that $\mathbf{q}_{B/D}$ converges to either $+\mathbf{1}$ or $-\mathbf{1}$. Note that $\mathbf{q}_{B/D} = +\mathbf{1}$ and $\mathbf{q}_{B/D} = -\mathbf{1}$ represent the same pose [10]. Therefore, either equilibrium is acceptable. However, this can lead to the so-called unwinding phenomenon, where a large rotation (greater than 180°) is performed despite the fact that a smaller rotation (less than 180°) exists. This problem of quaternions is well documented, and possible solutions exist in the literature [7].

REMARK 3 If the reference pose is constant—i.e., $\boldsymbol{\omega}_{D/I}^D = \mathbf{0}$ —then the pose-tracking controllers suggested in Theorems 1 and 2 become pose-stabilization controllers [12]. Note that in this special case, the feedback control laws (14) and (16) do not depend on M^B —i.e., they do not depend on the mass and inertia matrix of the rigid body.

REMARK 4 If A and B are chosen, respectively, as $-k_f I_{8 \times 8}$ and $k_f I_{8 \times 8}$ in (17), where $k_f > 0$, and the definition $Q = -k_d(B^{-T}A + A^T B^{-T})$ is adopted as in [14], the Kalman–Yakubovich–Popov conditions yield $P = k_d B^{-T}$ and $C = k_d I_{8 \times 8}$. Then the transfer-matrix representation of the LTI system (17) is given by $C_p(s) = ds/(s + a)$, where $d = k_d k_f$ and $a = k_f$. In this case, \mathbf{z} is obtained by differentiating $\mathbf{q}_{B/D}$ and passing $\dot{\mathbf{q}}_{B/D}$ through a low-pass filter. Theorem 2 proves that in the absence of measurement noise, the cutoff frequency of the low-pass filter can be chosen arbitrarily. In practice, in the presence of measurement noise, the cutoff frequency of the low-pass filter has to be chosen low enough to reject high-frequency measurement noise.

V. SIMULATION RESULTS

The velocity-feedback and the velocity-free pose-tracking controllers given by (14) and (16) are numerically verified and compared in this section via two examples. In the first example, a chaser spacecraft is required to track an elliptical motion around a target satellite while pointing at it. In the second example, the velocity-free controller is compared qualitatively and quantitatively to the velocity-feedback controller fed with velocity estimates produced by an EKF through a more realistic satellite proximity-operation simulation.

A. Satellite Proximity-Operation Example

The first example consists of a satellite proximity-operation scenario where a chaser satellite is required to track an elliptical motion around a target satellite while pointing at it.

Four reference frames are defined: the inertial frame, the target frame, the desired frame, and the body frame. The inertial frame is the Earth-centered inertial frame. The body frame is some frame fixed to the chaser satellite and centered at its center of mass. The target frame is defined as $\bar{I}_T = \bar{r}_{T/I} / \|\bar{r}_{T/I}\|$, $\bar{J}_T = \bar{K}_T \times \bar{I}_T$, and $\bar{K}_T = \bar{\omega}_{T/I} / \|\bar{\omega}_{T/I}\|$. The desired frame is defined as $\bar{I}_D = \bar{r}_{D/T} / \|\bar{r}_{D/T}\|$, $\bar{J}_D = \bar{K}_D \times \bar{I}_D$, and $\bar{K}_D = \bar{\omega}_{D/T} / \|\bar{\omega}_{D/T}\|$ [7]. The target satellite is assumed to be fixed to the target frame. The different frames are illustrated in Fig. 1. The control

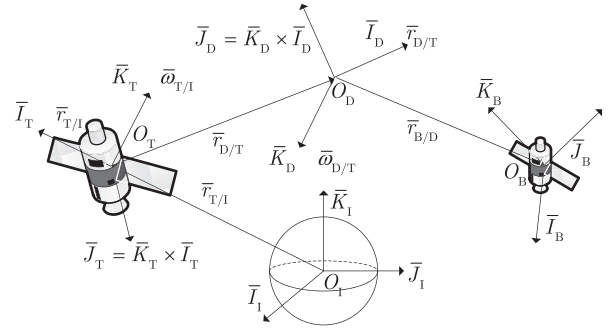


Fig. 1. Reference frames.

objective is to superimpose the body frame onto the desired frame.

The target spacecraft is assumed to be in a highly eccentric Molniya orbit with initial orbital elements given in [7] and nadir pointing. The relative motion of the desired frame with respect to the target frame is defined as an ellipse in the \bar{I}_T - \bar{J}_T plane with semimajor axis equal to 20 m along \bar{J}_T and semiminor axis equal to 10 m along \bar{I}_T . The relative orbit has constant angular speed equal to the mean motion of the target satellite. More precisely, during this phase, $\bar{\omega}_{D/T}^T = [0 \ 0 \ n]^T$ rad/s, $\bar{v}_{D/T}^T = [-a_e n \sin(nt) \ b_e n \cos(nt) \ 0]^T$ m/s, and $\bar{r}_{D/T}^T(0) = [a_e \ 0 \ 0]^T$ m, where $a_e = 10$ m, $b_e = 20$ m, $n = \sqrt{\mu/a^3}$ is the (unperturbed) mean motion of the target satellite, and a is the (unperturbed) semimajor axis of the target satellite.

The linear velocity of the target satellite with respect to the inertial frame is calculated by numerically integrating the gravitational acceleration [10, (73)] and the perturbing acceleration due to Earth's oblateness [10, (75)]. See [7] for expressions for the angular acceleration $\alpha_{T/I}^I$ of the target satellite with respect to the inertial frame expressed in the inertial frame and for expressions for the variables $\omega_{D/I}^D$ and $\dot{\omega}_{D/I}^D$.

In this example, the total external dual force acting on the chaser spacecraft is decomposed as $\mathbf{f}^B = \mathbf{f}_g^B + \mathbf{f}_{\nabla g}^B + \mathbf{f}_{J_2}^B + \mathbf{f}_c^B$, where \mathbf{f}_g^B is the gravitational force [10, (73)], $\mathbf{f}_{\nabla g}^B$ is the gravity gradient torque [10, (74)], $\mathbf{f}_{J_2}^B$ is the perturbing force due to Earth's oblateness [10, (75)], and \mathbf{f}_c^B is the dual control force. In turn, the dual control force is calculated as $\mathbf{f}_c^B = \mathbf{f}^B - \mathbf{f}_g^B - \mathbf{f}_{\nabla g}^B - \mathbf{f}_{J_2}^B$, where \mathbf{f}^B is given by either (14) or (16).

The mass and inertia matrix of the chaser satellite are assumed to be $m = 100$ kg and

$$\bar{I}^B = \begin{bmatrix} 22 & 0.2 & 0.5 \\ 0.2 & 20 & 0.4 \\ 0.5 & 0.4 & 23 \end{bmatrix} \text{ kg} \cdot \text{m}^2.$$

The initial conditions for this example are $\bar{r}_{B/D}^B(0) = [5 \ 5 \ 5]^T$ m, $\mathbf{q}_{B/D}(0) = (0.3320, [0.4618 \ 0.1917 \ 0.7999]^T)$,

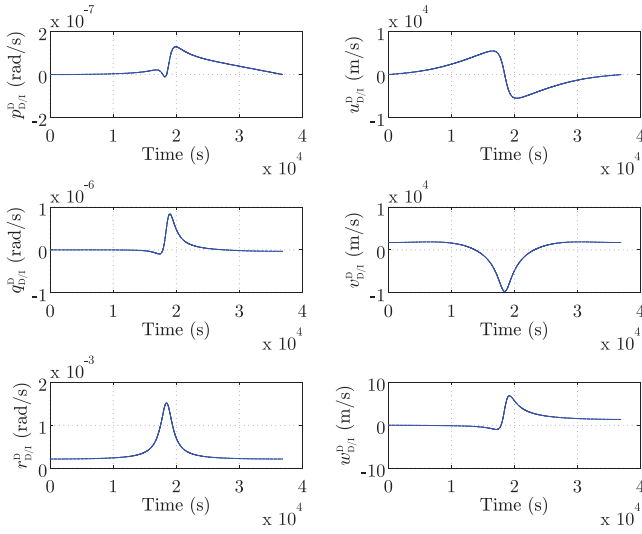


Fig. 2. Reference motion.

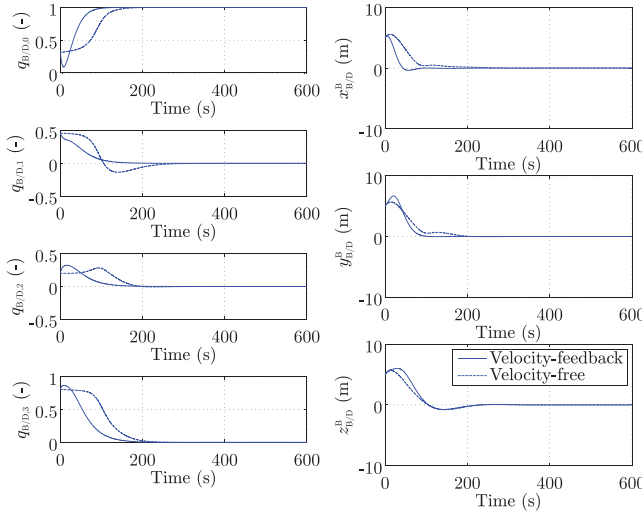


Fig. 3. Pose of body frame with respect to desired frame.

$\bar{v}_{B/D}^B(0) = [0.1 \ 0.1 \ 0.1]^T$ m/s, $\bar{\omega}_{B/D}^B(0) = [0.1 \ 0.1 \ 0.1]^T$ rad/s, and $\mathbf{x}_p(0) = \mathbf{q}_{B/D}(0)$.

The control gains are chosen as $k_p = 0.2$, in (14) and (16), and $k_d = 4$, in (14). The matrices of the LTI system are chosen as in Remark 4, with $k_f = 10$.

Fig. 2 shows the linear and angular velocity of the desired frame with respect to the inertial frame expressed in the desired frame for the complete maneuver. These signals represent the desired motion.

Fig. 3 shows the initial transient response of the pose of the body frame with respect to the desired frame obtained with the control laws with velocity feedback (14) and without velocity feedback (16). Both controllers are able to superimpose the body frame onto the desired frame after the initial transient response.

Fig. 4 shows the linear and angular velocity of the body frame with respect to the desired frame obtained with (14) and (16). Again, after the initial transient response, both controllers cancel the relative linear and angular velocity of the body frame with respect to the desired frame.

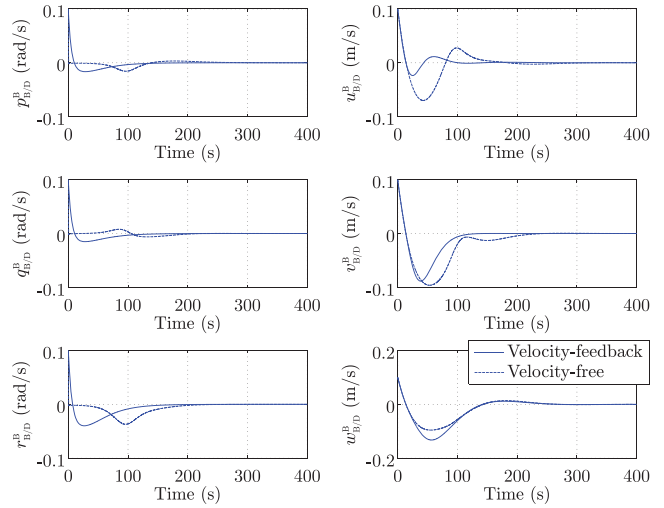


Fig. 4. Velocities of body frame with respect to desired frame.

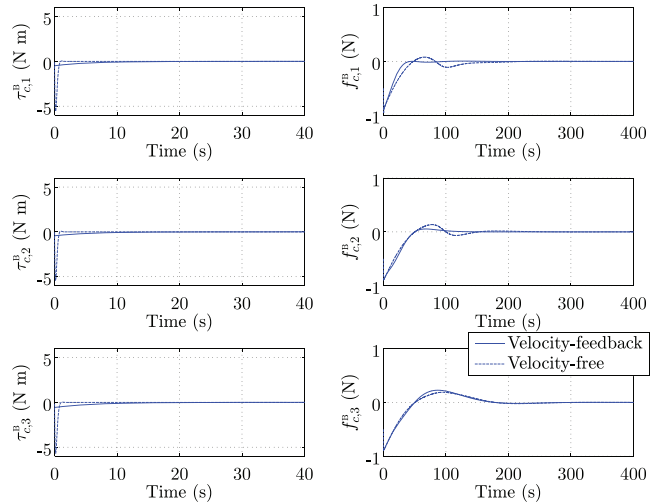


Fig. 5. Control force and torque during initial transient response.

Fig. 5 shows the control force and control torque during the initial transient response produced by (14) and (16). For completeness, Fig. 6 shows the control force and torque for the complete maneuver. As a comparison, the complete maneuver requires a ΔV of 0.6303 m/s if done with (14), with velocity feedback, and 0.0211 m/s more if done with (16), without velocity feedback.

B. Comparison Between the Velocity-Free Controller and the Velocity-Feedback Controller With EKF

Instead of using the velocity-free pose-tracking controller derived in Theorem 2 when measurements of $\omega_{B/D}^B$ are not available, one could use the velocity-feedback pose-tracking controller derived in Theorem 1 and an EKF to estimate the unmeasured $\omega_{B/D}^B$ from measurements of $\mathbf{q}_{B/D}$. The theoretical and numerical advantages and disadvantages of each solution are analyzed in this section.

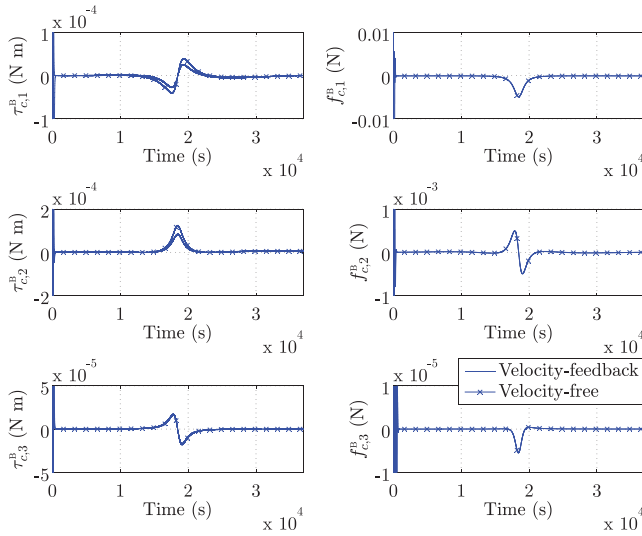


Fig. 6. Control force and torque during complete maneuver.

The first solution has three main advantages over the second solution. The first main advantage is that under the conditions specified in Theorem 2, pose tracking is guaranteed—i.e., $q_{B/D} \rightarrow \pm \mathbf{1}$ and $\omega_{B/D}^B \rightarrow \mathbf{0}$ as $t \rightarrow +\infty$ —independent of the initial condition chosen for \mathbf{x}_p . On the other hand, because an EKF is based on first-order approximations, if the initial guess of the state is not close enough to the true state, the EKF may diverge, causing the velocity-feedback controller to fail. The second main advantage of the velocity-free controller is that, according to Theorem 2, the LTI system in the feedback-loop can be designed independent of the value of k_p without violation of the almost globally asymptotic stability of the closed-loop system. On the other hand, there is no theoretical guarantee that the connection between the velocity-feedback controller derived in Theorem 1 and an EKF will ensure pose tracking. The third and final main advantage of the velocity-free controller is the smaller number of states. For example, whereas the velocity-free controller requires the propagation of eight states, the dual-quaternion multiplicative EKF (DQ-MEKF) described in [8] requires the propagation of 92 states to estimate $\omega_{B/D}^B$ from measurements of $q_{B/D}$ (mostly due to the propagation of the state covariance matrix). This might make the velocity-free controller more suitable for satellites with limited computational resources.

On the other hand, the solution based on the velocity-feedback controller and an EKF has three important advantages over the velocity-free controller. First, an EKF can handle measurement noise by design, whereas the model on which the velocity-free controller is based assumes no noise. Note, however that, for example, by choosing the matrices of the LTI system as in Remark 4, the user is free to choose the cutoff frequency of the low-pass filter in the feedback loop, which will help filter out measurement noise. Second, an EKF can be easily designed to handle discrete-time measurements, whereas the velocity-free controller described in Theorem 2

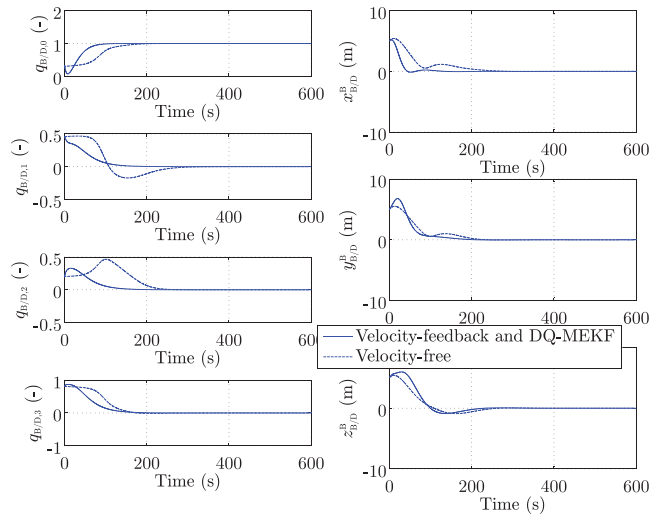


Fig. 7. Post tracking using velocity-free controller and velocity-feedback controller with DQ-MEKF.

assumes continuous-time measurements. Finally, an EKF can produce a direct estimate of $\omega_{B/D}^B$, whereas the velocity-free controller cannot. This estimate can be used to estimate $\omega_{D/I}^B = \omega_{B/I}^B - \omega_{B/D}^B$, which in turn is used in both (14) and (16). In an uncooperative satellite proximity-operation scenario, where $\omega_{D/I}^B$ is unknown, and assuming that the chaser satellite can measure its own linear and angular velocities with respect to the inertial frame—i.e., $\omega_{B/I}^B$ —this provides a method to estimate $\omega_{D/I}^B$, which is not available with the velocity-free controller. Most important, the EKF provides a measure of the uncertainty associated with the estimate of $\omega_{B/D}^B$ through the state covariance matrix.

To compare the two solutions numerically, both controllers were applied to the satellite proximity-operation scenario described in Section V-A, but now under more realistic conditions. Instead of continuous-time measurements, both controllers were now fed pose measurements at 10 Hz. Since the velocity-free controller requires continuous-time measurements, a zero-order hold was used to convert the discrete-time measurements into continuous-time signals. The EKF used in this comparison is the DQ-MEKF described in [8] that estimates $\omega_{B/D}^B$ from discrete-time measurements of the relative pose. Moreover, zero-mean additive white Gaussian noise is added to the measurements of $q_{B/D}$ and $r_{B/D}^B$, with standard deviations of, respectively, 1×10^{-4} and 1.7×10^{-3} m. After the additive white Gaussian noise is added to $q_{B/D}$, $q_{B/D}$ is renormalized through $q_{B/D} = (1/\|q_{B/D}\|)q_{B/D}$ [15]. Additionally, each element of the control torque and force is saturated at ± 5 N·m and ± 5 N, respectively. Also, the controllers are run at 100 Hz to simulate a satellite with limited computational resources. Finally, to make the comparison fair, the control gains are chosen as $k_p = 0.2$ and $k_d = 0.4$ both in (14) and in (16). All other parameters of the scenario are defined as in Section V-A.

Fig. 7 shows the initial transient response of the true (i.e., continuous-time and noise-free) pose of the body

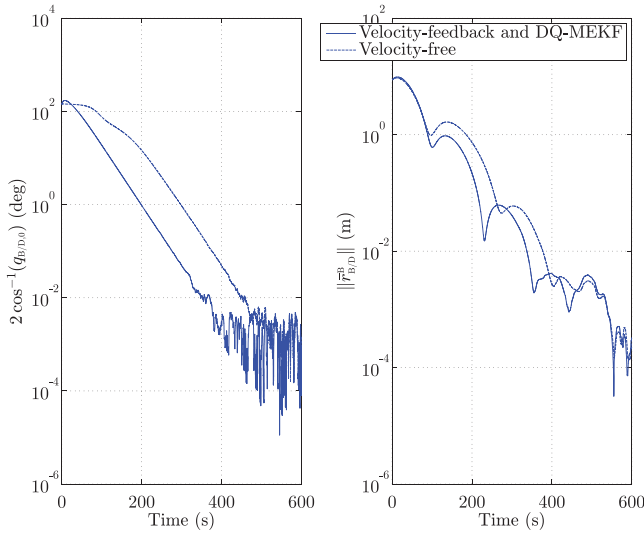


Fig. 8. Pose-tracking error using velocity-free controller and velocity-feedback controller with DQ-MEKF.

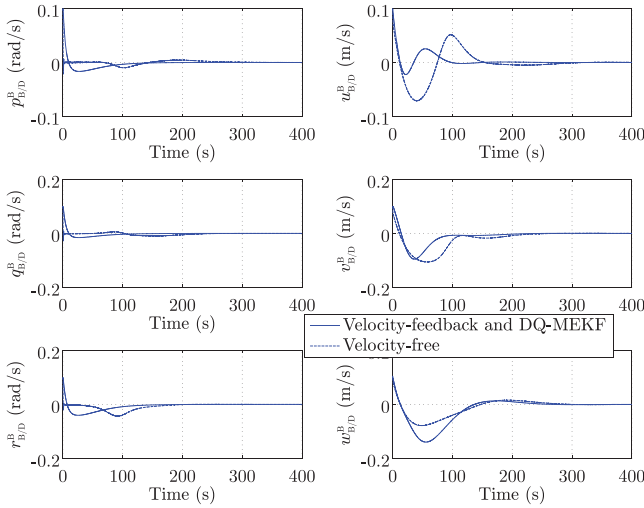


Fig. 9. Relative linear and angular velocity using velocity-free controller and velocity-feedback controller with DQ-MEKF.

frame with respect to the desired frame obtained with the velocity-free controller and with the velocity-feedback controller in series with the DQ-MEKF. It demonstrates that even under these more realistic conditions, both controllers can track the desired pose. In fact, Fig. 7 is relatively similar to Fig. 3, obtained under ideal conditions. The pose-tracking error is shown in more detail in Fig. 8. Whereas the pose-tracking error during the transient response is smaller with the velocity-feedback controller and the DQ-MEKF, both controllers achieve similar steady-state errors.

Fig. 9 shows the true (i.e., continuous-time and noise-free) linear and angular velocity of the body frame with respect to the desired frame obtained with both solutions under these more realistic conditions. Both controllers track the desired velocities. Again, note that Fig. 9 is relatively similar to Fig. 4, obtained under ideal conditions.

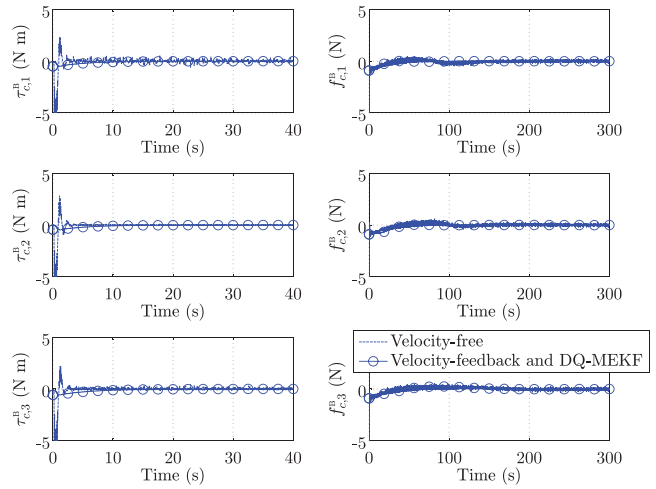


Fig. 10. Control force and torque using velocity-free controller and velocity-feedback controller with DQ-MEKF.

Finally, Fig. 10 shows the control force and torque produced by both controllers under these more realistic conditions. The control force and torque produced by the velocity-free controller exhibit noise and oscillations that are not visible in the control force and torque produced by the velocity-feedback controller with the DQ-MEKF. They also do not appear in Fig. 5 under ideal conditions. This is expected, since unlike the DQ-MEKF, the velocity-free controller does not filter out the measurement noise nor is designed to take discrete-time measurements.

Hence, in this particular scenario and assuming that the computational resources allow it, the velocity-feedback controller in series with the DQ-MEKF seems to be the more numerically robust solution to the pose-tracking problem without relative linear- and angular-velocity measurements. The velocity-free controller may be more suitable for small cheap satellites where operational requirements are not stringent and onboard computational resources are limited.

VI. CONCLUSION

This paper proposes a pose-tracking controller that guarantees almost globally asymptotic stability of the pose-tracking error even when relative linear- and angular-velocity measurements are not available. This property is proven for any reference pose with finite velocities and accelerations. The derivation of this controller is based on an existing attitude-tracking controller that guarantees almost globally asymptotic stability of the attitude-tracking error when angular-velocity measurements are not available and on the dual-quaternion formalism. The proposed controller is specially suited for uncooperative satellite proximity operations where the only relative measurements the chaser satellite has access to are relative pose measurements from, e.g., a vision-based sensor. The proposed controller is also useful in the case of malfunction of a velocity sensor. The simulation results

presented in this paper show that in a conceivable satellite proximity-operation scenario, the proposed velocity-free controller would require only 3% more ΔV than a controller that knows the true relative velocities. The simulation results presented in this paper also show that whereas using an EKF with a velocity-feedback controller can lead to better transient responses and controls than with the velocity-free controller (at least when the measurement noise is not carefully filtered in the latter solution), the additional 84 states required by the former solution might make the velocity-free controller a better option for satellites with limited computational resources.

ACKNOWLEDGMENT

The authors are grateful to the reviewers for insightful comments.

REFERENCES

- [1] Singla, P., Subbarao, K., and Junkins, J. L. Adaptive output feedback control for spacecraft rendezvous and docking under measurement uncertainty. *Journal of Guidance, Control, and Dynamics*, **29**, 4 (2006), 892–902.
- [2] Tanygin, S. Generalization of adaptive attitude tracking. In *AIAA/AAS Astrodynamics Specialist Conference and Exhibit*, Monterey, CA, Aug. 5–8, 2002, AIAA 2002-4833.
- [3] Wong, H., Pan, H., and Kapila, V. Output feedback control for spacecraft formation flying with coupled translation and attitude dynamics. In *Proceedings of the 2005 American Control Conference*, Portland, OR, June 8–10, 2005, **4**, 2419–2426.
- [4] Maithripala, D. H. S., Berg, J. M., and Dayawansa, W. P. Almost-global tracking of simple mechanical systems on a general class of Lie groups. *IEEE Transactions on Automatic Control*, **51**, 2 (Feb. 2006), 216–225.
- [5] Bhat, S. P., and Bernstein, D. S. A topological obstruction to continuous global stabilization of rotational motion and the unwinding phenomenon. *Systems & Control Letters*, **39**, 1 (2000), 63–70.
- [6] Filipe, N., and Tsiotras, P. Rigid body motion tracking without linear and angular velocity feedback using dual quaternions. In *2013 European Control Conference*. Zurich, Switzerland, July 17–19, **2013**, 329–334.
- [7] Filipe, N., and Tsiotras, P. Adaptive position and attitude-tracking controller for satellite proximity operations using dual quaternions. *Journal of Guidance, Control, and Dynamics*, **38**, 4 (2015), 566–577.
- [8] Filipe, N., Kontitsis, M., and Tsiotras, P. Extended Kalman filter for spacecraft pose estimation using dual quaternions. *Journal of Guidance, Control, and Dynamics*, **38** (2015), 1625–1641.
- [9] Akella, M. R. Rigid body attitude tracking without angular velocity feedback. *Systems & Control Letters*, **42**, 4 (2001), 321–326.
- [10] Filipe, N. R. S. Nonlinear pose control and estimation for space proximity operations: An approach based on dual quaternions. Ph.D. dissertation, Georgia Institute of Technology, Atlanta, 2014. Available: <http://hdl.handle.net/1853/53055>.
- [11] Haddad, W. M., and Chellaboina, V. *Nonlinear Dynamical Systems and Control: A Lyapunov-Based Approach*. Princeton, NJ: Princeton University Press, 2008.
- [12] Filipe, N., and Tsiotras, P. Simultaneous position and attitude control without linear and angular velocity feedback using dual quaternions. In *2013 American Control Conference*, Washington, DC, June 17–19, 2013, pp. 4808–4813.
- [13] Wen, J. T.-Y., and Kreutz-Delgado, K. The attitude control problem. *IEEE Transactions on Automatic Control*, **36**, 10 (Oct. 1991), 1148–1162.
- [14] Lizarralde, F., and Wen, J. T. Attitude control without angular velocity measurement: A passivity approach. *IEEE Transactions on Automatic Control*, **41**, 3 (Mar. 1996), 468–472.
- [15] Zanetti, R., Majji, M., Bishop, R. H., and Mortari, D. Norm-constrained Kalman filtering. *Journal of Guidance, Control, and Dynamics*, **32**, 5 (2009), 1458–1465.



Nuno Filipe is a guidance and control engineer in the NASA/Caltech Jet Propulsion Laboratory. Previously, he was a research and teaching assistant at the School of Aerospace Engineering of the Georgia Institute of Technology (GIT; 2010–2015) and a national trainee at the Control Systems Division of the European Space Agency (2008–2010). He has a Ph.D. degree in aerospace engineering from GIT, an M.Sc. degree in aerospace engineering from the Delft University of Technology, and a 5-year undergraduate degree in aerospace engineering from the Instituto Superior Técnico, Portugal. He is a recipient of the 2010–2013 International Fulbright Science and Technology Award and of the 2013 Best Graduate Student Technical Paper Award from the AIAA Guidance, Navigation, and Control Technical Committee. His Ph.D. degree thesis, titled *Nonlinear Pose Control and Estimation for Space Proximity Operations: An Approach Based on Dual Quaternions*, was selected as one of the 10 best of 2014 from GIT.



Alfredo Valverde is a Ph.D. degree student in the School of Aerospace Engineering at the Georgia Institute of Technology (GIT). His current research lies in the field of nonlinear control and estimation. He received his B.Sc. degree in aerospace engineering (2013) from GIT with highest honors, while holding research and teaching assistant positions in the aerospace-engineering and computer-science departments. He also received his M.Sc. degree in aerospace engineering (2014), with a specialization in the field of combustion and experimental research at the Aerospace Combustion Laboratory at GIT. He has held internship positions in the Guidance and Control Analysis group at JPL (2015) and at the Département Aérodynamique, Energétique et Propulsion at ISAE-SUPAERO (2012), and is actively involved in outreach programs for the enhancement of STEM education.



Panagiotis Tsiotras is the Dean's Professor in the School of Aerospace Engineering at the Georgia Institute of Technology. He received his engineering diploma in mechanical engineering from the National Technical University of Athens, Greece (1986), and his Ph.D. degree in aeronautics and astronautics from Purdue (1993). He also holds an M.S. degree in mathematics from Purdue. He has held visiting research appointments at MIT, JPL, INRIA Rocquencourt, and Mines ParisTech. His main research interests are in optimal and nonlinear control and vehicle autonomy. He has served on the editorial boards of *IEEE Transactions on Automatic Control*, *IEEE Control Systems Magazine*, *Journal of Guidance, Control, and Dynamics*, and the journal *Dynamics and Control*. He is a recipient of the NSF CAREER award, a Fellow of AIAA, and a Senior Member of IEEE.